Sains Malaysiana 45(8)(2016): 1213–1219

The Effect of $Al(NO_3)_3$ Concentration on the Formation of AuNPs using Low Temperature Hydrothermal Reaction for Memory Application

(Kesan Kepekatan $Al(NO_3)_3$ ke atas Pembentukan AuNPs dengan Menggunakan Tindak Balas Hidroterma Suhu Rendah untuk Aplikasi Ingatan)

S.A. NG, K.A. RAZAK*, K.Y. CHEONG, K.C. AW

ABSTRACT

Distribution of gold nanoparticles (AuNPs) on a substrate becomes crucial in nanotechnology applications. This work describes a route to fabricate AuNPs directly on silicon substrates by using an aluminum template in hydrothermal reaction at 80°C for 1 h. The effect of aluminum nitrate ($Al(NO_3)_3$) concentration in the hydrothermal bath was investigated. The properties of AuNPs were studied using field-emission scanning electron microscope (FESEM), x-ray diffractometer (XRD) and semiconductor characterization system (SCS). Two distinct sizes of AuNPs were observed by FESEM. XRD analysis proved the formation of AuNPs directly on the substrate. AuNPs were embedded between polymethylsilsesquioxane (PMSSQ) in order to investigate their effect on memory properties. The sample grown in 0.1 M $Al(NO_3)_3$ exhibited the largest hysteresis window (2.6 V) and the lowest V_{th} (2.2 V) to turn 'ON' the memory device. This indicated that good distribution of FCC structure AuNPs with 80±4 nm and 42±7 nm of large and small particles produced better charge storage capability. Charge transport mechanisms of AuNPs embedded in PMSSQ were explained in details whereby electrons from Si are transported across the barrier by thermionic effects via field-assisted lowering at the Si-PMSSQ interface with the combination of the Schottky and Poole Frenkel emission effect in Region 1. Trapped charge limited current (TCLC) and space charge limited current (SCLC) transport mechanism occurred in Region 2 and Region 3.

Keywords: Gold nanoparticles; hydrothermal; memory devices; template

ABSTRAK

Taburan nanopartikel emas (AuNPs) pada substrat adalah penting dalam aplikasi nanoteknologi. Kajian ini menerangkan cara untuk menghasilkan AuNPs secara langsung di atas substrat silikon dengan menggunakan templat aluminium dalam tindak balas hidroterma pada suhu 80°C selama 1 jam. Kesan kepekatan aluminium nitrat ($Al(NO_3)_3$) dalam rendaman hidroterma dikaji. Sifat AuNPs telah dikaji menggunakan pancaran medan mikroskop elektron imbasan (FESEM), pembelauan sinar-x (XRD) dan sistem pencirian semikonduktor (SCS). Dua saiz berbeza AuNPs diperhatikan menggunakan FESEM. Analisis XRD membuktikan pembentukan AuNPs secara langsung ke atas substrat. AuNPs tertanam antara polimetilsilseskuioksana (PMSSQ) untuk mengkaji kesannya ke atas sifat ingatan. Sampel yang dihasilkan di dalam 0.1 M $Al(NO_3)_3$ menghasilkan tetingkap histeresis terbesar (2.6 V) dan Vth (2.2 V) terendah untuk menghidupkan peranti ingatan. Ini menunjukkan pengagihan yang baik oleh struktur FCC AuNPs dengan 80±4 nm dan 42±7 nm partikel besar dan kecil menghasilkan keupayaan penyimpanan cas yang lebih baik. Mekanisme pengangkutan cas di dalam AuNPs tertanam dalam PMSSQ telah dijelaskan secara terperinci manakala elektron daripada Si diangkut merentasi halangan oleh kesan termionik melalui perendahan medan-berbantu pada antara muka Si-PMSSQ dengan gabungan kesan pancaran Schottky dan Poole Frenkel dalam Rantau 1. Mekanisme pengangkutan perangkap arus cas terhad (TCLC) dan ruang arus cas terhad (SCLC) berlaku di Rantau 2 dan 3.

Kata kunci: Hidroterma; nanopartikel emas; peranti ingatan; templat

INTRODUCTION

Nowadays, there has been increasing interest in the synthesis of gold nanoparticles (AuNPs) due to their potential applications in electrical, biological and medical (Granmayeh Rad et al. 2011; Kim et al. 2012; Liu et al. 2002). AuNPs have advantages of high work function, ease of synthesis route, good electron accepting properties and chemically stable. Besides, AuNPs have been used to enhance the conductivity of devices and storage properties in organic memory (Lee 2010). There were various methods which have been used to prepare AuNPs thin film on a substrate such as reduction or seedling growth method together with spin coating and self assembly method (Cao et al. 2006; Masala & Seshadri 2004; Philip 2008; Sun et al. 2002). However, for the spin coating method, AuNPs tend to agglomerate at the edge of substrate due to centrifugal effect (Das et al. 2008; Liu & Yu 2011; Sethuraman et al. 2008).

In the self assembly method, the substrate was functionalized first using chemicals with functional groups

in order to attract AuNPs to specific sites. However, oxygen plasma treatment was required to eliminate the chemicals that could cause the contamination of the memory device (Gowd et al. 2010; Haensch et al. 2010; Thanh & Green 2010). Other than that, AuNPs can be produced by heat treatment of sputtered gold thin film through diffusion approach. But this method is not suitable because the size and number of AuNPs cannot be controlled (Daniel & Astruc 2004). AuNPs can be synthesized through Langmuir-Blodgett film deposition, but this method required complicated processing steps and several chemical reactions (Paul et al. 2003).

Previously, we reported direct formation of AuNPs on a substrate using a sacrificial template hydrothermal method (Goh et al. 2012; Ng et al. 2014). In the sacrificial hydrothermal method, AuNPs were grown directly on high energy sites between the grains of the template. This approach provides the most convenient, low cost and attractive routes to fabricate *in situ* generation of the AuNPs directly on the substrate. In previous works (Goh et al. 2012; Ng et al. 2014), we studied the formation of AuNPs using Zn template only. However, the effects of precursors in hydrothermal bath have not been studied yet. In this work, sputtered Al template was utilized as a template and the effects of $Al(NO_3)_3$ concentration was studied.

Organic memory device embedded with nanostructure materials as the charge trapping centres become of interest in recent years because of their high current density, large ON/OFF current ratio and other great performance (Kim et al. 2012). In order to study the electrical properties of AuNPs for memory devices, the metal-insulator-semiconductor (MIS) structure consisting of metal/ tri-layer/ semiconductor was fabricated in this study. The tri-layer stacking structure (polymer/ metallic nanoparticles/ polymer) is very important for charge trapping to occur. The charge storage capability of AuNPs which were embedded in insulating layer is beneficial as a memory device. Therefore, the memory properties of AuNPs embedded in PMSSQ was explained accordingly in this study.

Methods

In this work, a memory device structure with AuNPs grown by the sacrificial hydrothermal method embedded in polymethylsilsesquioxane (PMSSQ) dielectric was fabricated. The n-type <100> silicon wafer of 1 × 1 cm substrates were cleaned using a standard Radio Corporation of America (RCA) cleaning procedure to remove organic and inorganic contaminants. The RCA cleaning consists of the following steps: First step involved organic cleaning with 1:1:5 volume ratio mixture of 37% hydrogen peroxide: 28% ammonium hydroxide: distilled water. Si substrates were immersed in the solution at 80°C for 10 min. After that the substrates were rinsed in distilled water. Second step involved removal of oxide on the Si substrates by soaking the 1:50 of hydrofluoric acid and distilled water in a polypropylene beaker, then rinsed with distilled water. Then, ionic cleaning was performed in a 1:1:6 volume ratio mixture of 49% hydrochloric acid: 37% hydrogen peroxide: distilled water in which the Si substrates were immersed in the solution at 80°C for 10 min. The substrates were then rinsed with distilled water. The substrates were left in distilled water for 5 min and dried using nitrogen gas.

250 nm polymethylsilsesquioxane (PMSSQ 1) was deposited using a spin coating at 2000 rpm for 100 s. Then, the samples were cured at 160°C for 1 h to cure the PMSSQ. Then Al templates were deposited using a DC sputtering method on the PMSSQ/Si substrates. The AuNPs were grown on the Al template by using the sacrificial hydrothermal approach. The Al/PMSSQ/Si substrates were then subjected to hydrothermal reaction in a pre-heated oven at 80°C for 1 h. The hydrothermal bath contained aluminum nitrate tetrahydrate ($Al(NO_3)_3.9H_2O$), 0.1M hexamethylenetetramine ($C_6H_{12}N_4$), 0.01M gold (III) chloride trihydrate ($AuCl_4.3H_2O$) and 10 mL acetic acid. Al $(NO_3)_3$ concentration in the hydrothermal bath was varied: 0.01M, 0.05M, 0.1M and 0.2M. After hydrothermal reaction, the samples were removed and rinsed with deionised water. Then, the samples were heat treated at 160°C for 30 min in an oven in order to obtain good adhesion of AuNPs. The samples were then characterized using field-emission scanning electron microscope (FESEM) (LEO Gemini) equipped with energy dispersive x-ray spectrometer (EDX) (ZEISS SUPRA™ 35VP). The phases presence in the samples were analyzed using x-ray diffractometer (XRD) (Bruker D8). For electrical properties analysis, a second layer of PMSSQ 2 was spin coated on the grown AuNPs and cured at 160°C for 1 h. A gold top and aluminum bottom contacts were deposited using the thermal evaporation method with the aid of a shadow mask. The memory characteristics (*C-V* and *I-V*) of the device were examined and measured using semiconductor characterization system Keithley Model 4200-SCS.

Results and Discussion

$HAuCl_4$ and $Al(NO_3)_3$ are the oxidizing agents (Gupta et al. 2014; Taleghani & Riahi-Noori 2013) which undergoes reduction with the reducing agents; HMT and acetic acid, in the chemical reaction. A competitive reaction occurs in the sacrificial hydrothermal process in this work. AuNPs formation (1) is more favorable and thus the Al_2O_3 formation in (2) is suppressed due to Gibbs energy (ΔG) value on formation of AuNPs is -604.7 kJ/mol which can proceed spontaneously compared to the ΔG value on formation of Al_2O_3 which is -226.48 kJ/mol (Raznjevic 1976).

$$HAuCl_4 + OH^- + 4H^+ \text{---> } Au + H_2O + 4HCl \quad (1)$$

$$Al(NO_3)_3.9H_2O + Al^{3+} + 6OH^- + 3H^+ \text{---> } Al_2O_3 + 3H_2O \quad (2)$$

In this work, the effects of $Al(NO_3)_3$ concentration on the formation of AuNPs using hydrothermal method were investigated. Figure 1 shows the FESEM images of AuNPs grown with various $Al(NO_3)_3$ concentration in hydrothermal precursor using Al template. Two distinct sizes of AuNPs were obtained from the FESEM images. This is due to the rate of reduction for AuNPs formation. For instance, the formation of larger particles is due to the fast reduction process of $HAuCl_4$ which led to the formation of heterogeneous population of AuNPs (Mantri et al. 2013). The average particle size and area density of each sample were calculated from FESEM images using ImageJ software as tabulated in Table 1. AuNPs grown in 0.01 M $Al(NO_3)_3$ concentration shown in Figure 1 contains 90±8 and 57±7 nm of large and small particle size, with 2.71 and 1.73×10^{12} m^{-2} area density of AuNPs distribution, respectively. The AuNPs formation involves chemical reactions between $Al(NO_3)_3$ and $HAuCl_4$ with reducing agent. Low amount of $Al(NO_3)_3$ reacts with the reducing agent causes the presence of excess reducing agent that can react with $HAuCl_4$ and forms various shapes of AuNPs as shown in Figure 1(a). This was in agreement with Ward et al. (2014) findings that excess reducing agent formed none spherical AuNPs such as triangle, trapezoidal, cubic, hexagonal and rods.

Large and small particles size of AuNPs growth in 0.05 M $Al(NO_3)_3$ concentration decreased to 83±7 and 52±6 nm. The area density of AuNPs growth in 0.05 M $Al(NO_3)_3$ concentration for large particles decrease and small particles increase to 2.38×10^{12} m^{-2}. In 0.1 M $Al(NO_3)_3$, the large and small size of AuNPs for the sample synthesized were 80±4 and 42±7 nm, respectively. This parameter produced good distribution of large and small AuNPs with area density of 1.29 and 2.71×10^{12} m^{-2}, respectively, due to sufficient reducing agent in the precusor reacts with the $HAuCl_4$ after the reducing agent have been reacted with the oxidative $Al(NO_3)_3$ to form monodispersed spherical AuNPs. However the AuNPs formed in 0.05M $Al(NO_3)_3$ produced more spherical particle of AuNPs compared to 0.1M $Al(NO_3)_3$, the distribution of AuNPs formed in 0.05M $Al(NO_3)_3$ precursor is not well dispersed and the existence of some agglomerated AuNPs was observed.

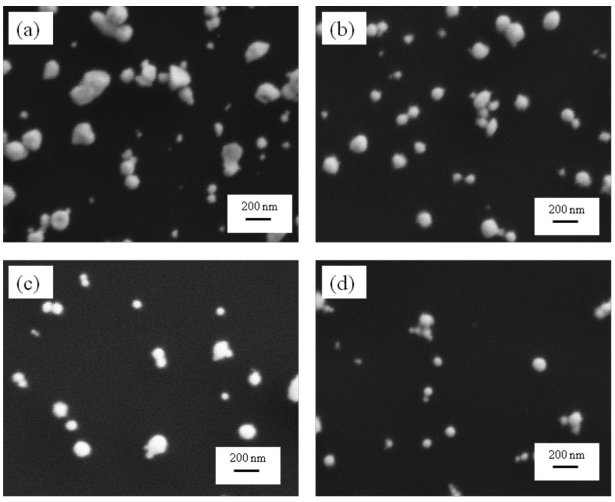

FIGURE 1. FESEM images of AuNPs grown with varying $Al(NO_3)_3$ concentration: (a) 0.01M, (b) 0.05 M, (c) 0.1M, (d) 0.2 M

The size of large AuNPs prepared in 0.20 M $Al(NO_3)_3$ concentration became smaller with only 75±7 nm and less particles distribution with 1.08×10^{12} m^{-2} area density. Meanwhile, the particles size and area density of small AuNPs were 50±9 nm and 3.36×10^{12} m^{-2} in the sample. When comparing the size of AuNPs, the size decreased with increasing $Al(NO_3)_3$ concentration. This is because when the concentration of $Al(NO_3)_3$ increases, more reducing agent reacts with the strong oxidative $Al(NO_3)_3$ that cause insufficient amount of reducing agent in reduction of $HAuCl_4$ to form AuNPs. Hence, it will limit the function of reducing agent as capping agent and thus the Van der Waals attractive force acts as a driving force for integration of AuNPs resulting in the formation of aggregated AuNPs. This finding was in agreement with the finding that Van der Waals force causes the nanoparticles form in chain and aggregates structure when salt concentration increases (Mark 2013).

The XRD spectra of AuNPs after hydrothermal reaction are shown in Figure 2. The peaks can be ascribed to Face-centered cubic (FCC) (JCPDS No.04-0784). The diffraction appeared at $2\theta = 38.20°$, 44.41° and 64.54° which respectively were corresponding to the (111), (200) and (220) planes of the standard Au cubic. Meanwhile, Si peaks appeared came from the Si substrate and PMSSQ layers. The Al peak disappeared after hydrothermal reaction due to competitive growth between Al and Au. AuNPs formation was more favorable and thus the Al formation was suppressed. Moreover, Al peak did not exist in XRD spectra after AuNPs formation proved that Al template was completely dissolved during hydrothermal reaction due to the acidicity of hydrothermal bath which is pH2 that could dissolve the Al thin film. This finding was also observed by

TABLE 1. Size and particles density of AuNPs grown with varying $Al(NO_3)_3$ concentration

$Al(NO_3)_3$ concentration (M)	Size		Area density	
	Large (nm)	Small (nm)	Large (m^{-2})	Small (m^{-2})
0.01	90±8	57±7	2.71×10^{12}	1.73×10^{12}
0.05	83±7	52±6	2.38×10^{12}	2.38×10^{12}
0.10	80±4	42±7	1.29×10^{12}	2.71×10^{12}
0.20	75±7	50±9	1.08×10^{12}	3.36×10^{12}

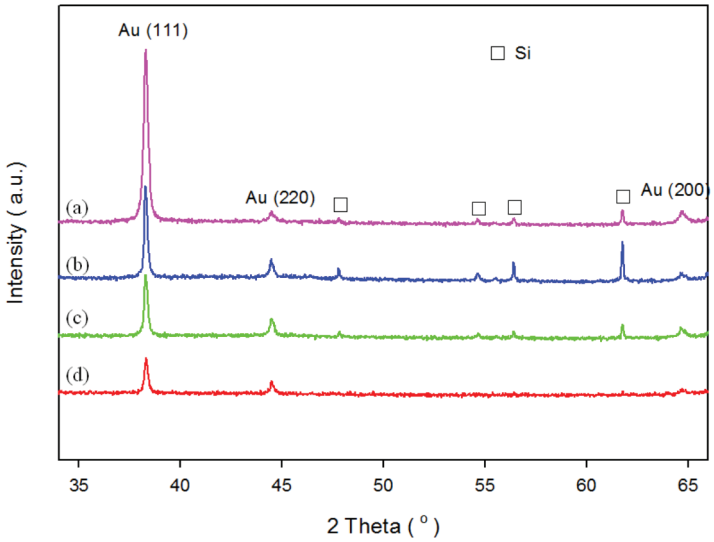

FIGURE 2. XRD spectra of AuNPs grown with varying $Al(NO_3)_3$ concentration (a) 0.01M, (b) 0.05 M, (c) 0.1 M and (d) 0.2 M

Hassan et al. (2013). Al template dissolves in the acid to form salts that contain Aluminum (III) cation, Al^{3+}. The ΔG value is -970.68 kJ/mol, thus chemical reaction proceeds spontaneously in the forward direction to dissolve the Al template due to negative value in (3) (Raznjevic 1976).

$$2Al + 6H^{+} \text{---> } 2Al^{3+} + 3H_2 \quad (3)$$

The average crystallite size was calculated using the Scherrer equation in (4) using (111), (220) and (200) reflection peaks.

$$d = \frac{0.89\lambda}{\beta \cos\theta} \quad (4)$$

where λ is the x-ray beam wavelength (= 1.54 Å for Cu Kα); β is the full width at half maximum (FWHM) of the Bragg peak; and θ is the peak position. The crystallite size is tabulated in Table 2. Crystallite size of AuNPs grown using 0.01, 0.05, 0.1 and 0.2 M $Al(NO_3)_3$ are 531.4, 433.8, 399.7 and 286.4 Å, respectively. This finding was in agreement with SEM observation (Figure 1) whereby the size of AuNPs decreases with increasing $Al(NO_3)_3$ concentration. In crystallite size calculation, the peak obtained using XRD is average diffraction from both large and small particles.

For current-voltage (*I-V*) measurement, a layer of PMSSQ was spin coated on the AuNPs. The top Au and bottom Al contacts were prepared using the thermal evaporation technique, respectively. The *I-V* characteristics of PMSSQ embedded AuNPs with various $Al(NO_3)_3$ concentration in hydrothermal reaction are shown in Figure 3. The *I-V* characteristics were obtained by applying a positive voltage and swept from 0 to 10 V and vice versa. The *I-V* characteristics in Figure 3 were marked as Regions 1, 2 and 3 to explain the possible transport mechanisms for the memory device structure. The *I-V* relationship was expressed as $I \alpha V_n$, and the slope value was determined. An abrupt current increment was observed at the threshold voltage (V_{th}) in Region 2 during the forward sweep.

In Figure 3, the curve at low voltage which is Region 1, the thermionic emission (TE) current conduction occurred at low voltage, which was related to the thermally generated electrons because TE is a process by which heat induces the emission of electrons across a barrier. At the same time, the transport mechanism is considered as Schottky and Poole Frenkel emissions because the electron is possible to be transported over the Si-PMSSQ interface via Schottky emission and Poole–Frenkel emission in the 250 nm thick of porous silicate PMSSQ and it is well fitted to log (I/T_2) α $V_{0.5}$ and log (I/V) α $V_{0.5}$, respectively. Therefore, electrons from Si are transported across the barrier by thermionic

TABLE 2. Crystallite size of AuNPs grown with varying concentration of $Al(NO_3)_3$ precursor

$Al(NO_3)_3$ concentration (M)	Crystallite size (Å)			Average crystallite size
	(111)	(220)	(200)	
0.01	496.8	637.1	463.2	531.4
0.05	496.8	519.9	284.8	433.8
0.10	414.2	507.0	277.8	399.7
0.20	310.7	317.0	231.5	286.4

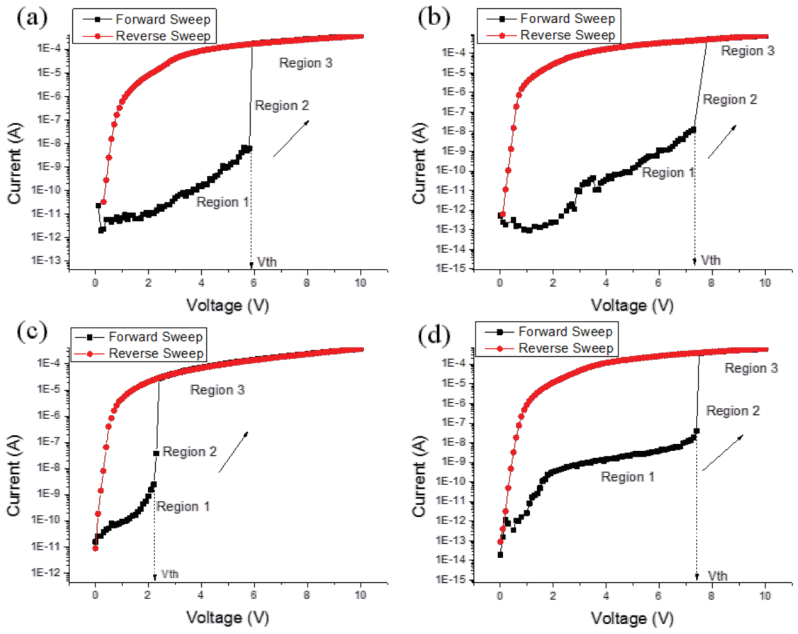

FIGURE 3. *I-V* measurement of AuNPs grown with varying $Al(NO_3)_3$ concentration (a) 0.01 M, (b) 0.05 M, (c) 0.1 M and (d) 0.2 M

effects via field-assisted lowering at the Si-PMSSQ interface with the combination of the Schottky and Poole Frenkel emission effect. When the voltage was increased to V_{th}, the transport mechanism switched to the trapped charge limited current (TCLC) for all memory devices due to n>>2 was obtained in Region 2. In this region, the trap sites from the presence of AuNPs started to be filled by electrons and an abrupt increase in current was observed. After all traps in the AuNPs were filled, the transport mechanism switched to trap-free space charge limited current (an ideal SCLC transport mechanism has n = 2) for all cases in Region 3. The transport mechanism was in agreement with Lai et al. (2013) findings. When the voltage was swept to the reverse condition (10 to 0 V), the current flow through the device remain high due to the traps were fully filled with electrons and in SCLC transport mechanism. The existence of the memory effect was proven as the electrons could be stored when the AuNPs dispersed randomly in the insulating PMSSQ layer by capturing the electrons which were injected from electrodes.

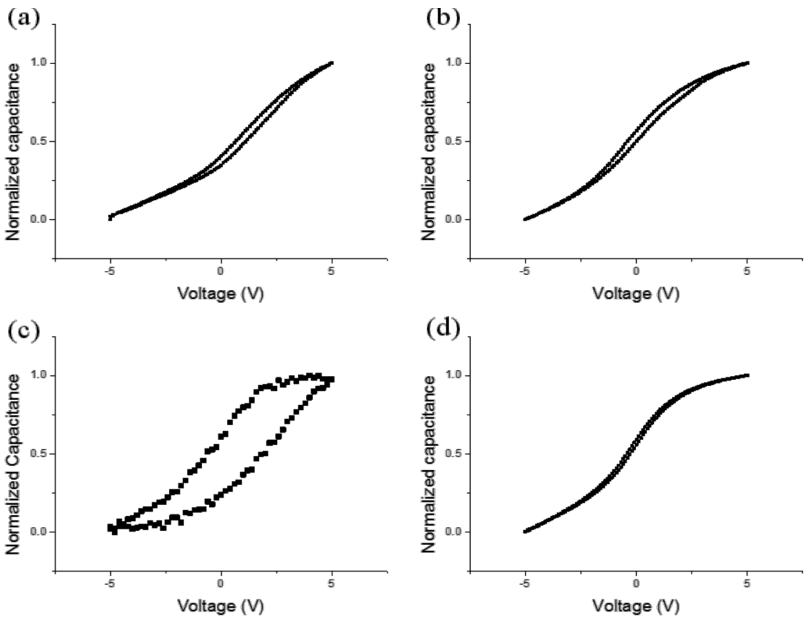

FIGURE 4. *C-V* measurement of AuNPs grown with varying $Al(NO_3)_3$ concentration (a) 0.01 M, (b) 0.05 M, (c) 0.1 M and (d) 0.2 M

The capacitance voltage (*C-V*) characteristics of the PMSSQ embedded AuNPs which were prepared with various concentration of $Al(NO_3)_3$ were shown in Figure 4. Prior to further investigation of the AuNPs effects on metal-insulator-semiconductor (MIS) structure, the negligible charge-trapping capability without AuNPs between PMSSQ for the *C-V* hysteresis windows has been reported previously (Ahmad et al. 2011). For the reverse sweep, the current increased in all memory devices due to the trapped electrons in the AuNPs sites (Park et al. 2008). The hysteresis (flat-band voltage shift, ΔV_{FB}) window for the sample prepared in the 0.1 M concentration of $Al(NO_3)_3$ was 2.6 V which exhibited the largest hysteresis compared to other concentrations of $Al(NO_3)_3$ in the precursor whereby just negligible value of hysteresis window formed due to well isolated distribution of AuNPs in 0.1 M concentration of $Al(NO_3)_3$. Therefore, the sample of AuNPs prepared using 0.1 M concentration of $Al(NO_3)_3$ exhibited the best memory effect by storing more electrons.

CONCLUSION

AuNPs were successfully grown on sputtered Al templates using the sacrificial hydrothermal method. The size and distribution of AuNPs were dependent on $Al(NO_3)_3$ concentration. The FCC structure AuNPs grown in 0.1 M $Al(NO_3)_3$ with 80±4 and 42±7 nm of large and small particles size produced the best memory properties. This optimum parameter with good distribution of AuNPs produced the lowest turn 'ON' value of 2.2 V and the largest hysteresis loop of 2.6 V which can store more charges in the memory devices.

ACKNOWLEDGMENTS

The authors appreciate the technical assistance of the School of Materials & Mineral Resources Engineering, Institute for Research in Molecular Medicine and Nano Optoelectronics Research Lab, Universiti Sains Malaysia. This research was jointly supported by the Postgraduate Research Grant Scheme 1001/PBAHAN/8046031 and Scholarship MyPhD.

REFERENCES

Ahmad, Z., Ooi, P.C., Aw, K.C. & Sayyad, M.H. 2011. Electrical characteristics of poly(Methylsilsesquioxane) thin films for non-volatile memory. *Solid State Communications* 151(4): 297-300.

Cao, L., Zhu, T. & Liu, Z. 2006. Formation mechanism of nonspherical gold nanoparticles during seeding growth: Roles of anion adsorption and reduction rate. *Journal of Colloid and Interface Science* 293(1): 69-76.

Daniel, M.C. & Astruc, D. 2004. Gold nanoparticles: Assembly, supramolecular chemistry, quantum-size-related properties, and applications toward biology, catalysis, and nanotechnology. *Chemical Reviews* 104(1): 293-346.

Das, A., Das, S. & Raychaudhuri, A.K. 2008. Growth of two-dimensional arrays of uncapped gold nanoparticles on silicon substrates. *Bulletin of Materials Science* 31(3): 277-282.

Goh, L., Razak, K., Ridhuan, N., Cheong, K., Ooi, P. & Aw, K. 2012. Direct formation of gold nanoparticles on substrates using a novel zno sacrificial templated-growth hydrothermal approach and their properties in organic memory device. *Nanoscale Research Letters* 7(1): 563.

Gowd, E.B., Nandan, B., Bigall, N.C., Eychmüller, A., Formanek, P. & Stamm, M. 2010. Hexagonally ordered arrays of metallic nanodots from thin films of functional block copolymers. *Polymer* 51(12): 2661-2667.

Granmayeh Rad, A., Abbasi, H. & Afzali, M.H. 2011. Gold nanoparticles: Synthesising, characterizing and reviewing novel application in recent years. *Physics Procedia* 22: 203-208.

Gupta, B., Melvin, A. & Prakash, R. 2014. Synthesis of polyanthranilic acid-au nanocomposites by emulsion polymerization: Development of dopamine sensor. *Bulletin of Materials Science* 37(6): 1389-1395.

Haensch, C., Hoeppener, S. & Schubert, U.S. 2010. Chemical modification of self-assembled silane based monolayers by surface reactions. *Chemical Society Reviews* 39(6): 2323-2334.

Kim, T.W., Yang, Y., Li, F. & Kwan, W.L. 2012. Electrical memory devices based on inorganic/organic nanocomposites. *NPG Asia Materials* 4: e18.

Lai, Y.C., Wang, D.Y., Huang, I.S., Chen, Y.T., Hsu, Y.H., Lin, T.Y., Meng, H.F., Chang, T.C., Yang, Y.J., Chen, C.C., Hsu, F.C. & Chen, Y.F. 2013. Low operation voltage macromolecular composite memory assisted by graphene nanoflakes. *Journal of Materials Chemistry C* 1(3): 552-559.

Lee, J.S. 2010. Recent progress in gold nanoparticle-based non-volatile memory devices. *Gold Bulletin* 43(3): 189-199.

Liu, C.H. & Yu, X. 2011. Silver nanowire-based transparent, flexible, and conductive thin film. *Nanoscale Res. Lett.* 6(1): 75.

Mantri, K., Selvakannan, P., Tardio, J. & Bhargava, S.K. 2013. Synthesis of very high surface area au-sba-15 materials by confinement of gold nanoparticles formation within silica pore walls. *Colloids and Surfaces A: Physicochemical and Engineering Aspects* 429: 149-158.

Mark, P.R. 2013. Forces and interactions between nanoparticles for controlled structures. PhD Thesis. Rutgers University-Graduate School-New Brunswick (Unpublished).

Masala, O. & Seshadri, R. 2004. Synthesis routes for large volumes of nanoparticles. *Annu. Rev. Mater. Res.* 34: 41-81.

Ng, S.A., Razak, K.A., Goh, L.P., Cheong, K.Y., Ooi, P.C. & Aw, K.C. 2014. Direct formation of aunps thin film using thermal evaporated zinc as sacrificial template in hydrothermal method. *Journal of Materials Science: Materials in Electronics* 25(5): 2227-2236.

Park, B., Im, K.J., Cho, K. & Kim, S. 2008. Electrical characteristics of gold nanoparticle-embedded mis capacitors with parylene gate dielectric. *Organic Electronics* 9(5): 878-882.

Paul, S., Pearson, C., Molloy, A., Cousins, M., Green, M., Kolliopoulou, S., Dimitrakis, P., Normand, P., Tsoukalas, D. & Petty, M. 2003. Langmuir-Blodgett film deposition of metallic nanoparticles and their application to electronic memory structures. *Nano Letters* 3: 533-536.

Philip, D. 2008. Synthesis and spectroscopic characterization of gold nanoparticles. *Spectrochimica Acta Part A: Molecular and Biomolecular Spectroscopy* 71(1): 80-85.

Raznjevic, K. 1976. Handbook of Thermodynamic Tables and Charts. Philadelphia: Hemisphere Publishing Corporation.

Sethuraman, K., Ochiai, S., Kojima, K. & Mizutani, T. 2008. Performance of poly(3-hexylthiophene) organic field-effect transistors on cross-linked poly(4-vinyl phenol) dielectric layer and solvent effects. *Applied Physics Letters* 92(18): 183302.

Sun, X., Fu, Z. & Wu, Z. 2002. Fractal processing of afm images of rough zno films. *Materials Characterization* 48(2-3): 169-175.

Taleghani, M. & Riahi-Noori, N. 2013. Synthesis of alumina nano powder by a gel combustion method. *Journal of Ceramic Processing Research* 14(1): 17-21.

Thanh, N.T. & Green, L.A. 2010. Functionalisation of nanoparticles for biomedical applications. *Nano Today* 5(3): 213-230.

Ward, C.J., Tronndorf, R., Eustes, A.S., Auad, M.L. & Davis, E.W. 2014. Seed-mediated growth of gold nanorods: limits of length to diameter ratio control. *Journal of Nanomaterials* 2014: Article ID 765618.

S.A. Ng, K.A. Razak* & K.Y. Cheong
School of Materials and Mineral Resources Engineering
Universiti Sains Malaysia
14300 Nibong Tebal, Pulau Pinang
Malaysia

K.A. Razak*
NanoBiotechnology Research and Innovation
INFORMM, Universiti Sains Malaysia
11800 Pulau Pinang
Malaysia

K.C. Aw
Mechanical Engineering
The University of Auckland, Auckland
New Zealand

*Corresponding author; email: khairunisak@usm.my

Received: 20 April 2015
Accepted: 18 November 2015